Journal of Magnetics 6(4), 132-141 (2001)

Computer Simulation of Switching Characteristics and Magnetization Flop in Magnetic Tunnel Junctions Exchange Biased by Synthetic Antiferromagnets

Y. R. Uhm and S. H. Lim*

Future Technology Research Division, Korea Institute of Science and Technology, P.O. Box 131, Cheongryang, Seoul 130-650, Korea

(Received 2 March 2001)

The switching characteristics and the magnetization-flop behavior in magnetic tunnel junctions exchange biased by synthetic antiferromagnets (SyAFs) are investigated by using a computer simulations based on a single-domain multilayer model. The bias field acting on the free layer is found to be sensitive to the thickness of neighboring layers, and the thickness dependence of the bias field is greater at smaller cell dimensions due to larger magnetostatic interactions. The resistance to magnetization flop increases with decreasing cell size due to increased shape anisotropy. When the cell dimensions are small and the synthetic antiferromagnet is weakly, or not pinned, the magnetization directions of the two layers sandwiching the insulating layer are aligned antiparallel due to a strong magnetostatic interaction, resulting in an abnormal magneto resistance (MR) change from the high-MR state to zero, irrespective of the direction of the free-layer switching. The threshold field for magnetization-flop is found to increase linearly with increasing antiferromagnetic exchange coupling in the synthetic antiferromagnet. Irrespective of the magnetic parameters and cell sizes, magnetization flop does not exist near zero applied field, indicating that magnetization flop is driven by the Zeeman energy.

Key words : magnetic tunnel junctions, magnetization switching, magnetization-flop, size effects, magnetostatic interactions, computer simulation.

1. Introduction

Since the first experimental realization of large room-temperature magnetoresistance (MR) in magnetic tunnel junctions (MTJs) in 1995 [1, 2], much progress has been made in this field [3-6]. It is now possible to fabricate junctions with very high MR values (~50%) and to control the value of the junction resistance through a precise control of the thickness and the characteristics of the oxide layer. Other important achievements include the process technology by which very uniform values of MR and junction resistance can be obtained on a wafer level, and thermal stability up to 300 °C. These achievements are expected to contribute significantly to the successful realization of a commercially viable magnetic random access memory (MRAM). An MTJ-based MRAM is known to possess many good intrinsic characteristics as a memory cell, some of which include nonvolatility, high density (comparable to DRAM) and speed (comparable to SRAM), and unlimited read/write operation [4]. From the practical point of view, it is important to realize high density, among many other things, in order for an MRAM to compete with other existing technologies. At a practical density level, the cell dimensions are expected to be in the submicron size range, where the switching of a magnetic layer is dominated by magnetostatic interactions. Switching fields are related to two characteristic magnetic fields: the bias field and the coercivity. This indicates that the switching characteristics can be understood through a detailed knowledge of these two magnetic parameters.

Two separate field components, the self-demagnetizing field and the interlayer magnetostatic interaction field, can be identified from the magnetostatic interactions, and it was shown previously in a single-domain multilayer model that the coercivity and the bias field are completely explained, respectively, by the self-demagnetizing field and the interlayer magnetostatic interaction field [7]. The self-demagnetizing field is determined by two factors, the self-demagnetizing coefficient and the saturation magnetization, the former being only a function of the geometry (dimensions, including the aspect ratio) of a magnetic layer. This indicates that the self-demagnetizing field (and, hence, the coercivity) of a magnetic layer is dependent on the related properties of the magnetic layer itself under consideration, but is independent of the multilayer structure (or design). On the other hand, the interlayer magnetostatic interaction field, which is caused by stray fields from neighboring lay-

*Corresponding Author: Tel: +82-2-958-5415, Fax: +82-2-958-6851, e-mail: sangho@kist.re.kr

ers, depends on the structure of a multilayer. In conventional MTJs, where the pinned layer is exchange-biased by a single layer of an antiferromagnet (AF) (FeMn, for example), the stray field from the pinned layer plays the role of biasing the free layers causing a hysteresis loop asymmetry. The switching asymmetry becomes very large at submicron cell dimensions [7]. This problem can be relieved, if not solved, by substituting a synthetic antiferromagnet (SyAF) for a single AF layer. Currently popular SyAFs are Co/Ru/Co [8] and Co/Ru/Co/AF (such as FeMn) [3, 9]. In this structure, a large portion of the stray field radiating from one of the Co layers is absorbed by the other Co layer, minimizing the stray field reaching the free layer.

In spite of the many merits of a SyAF, a potentially serious problem may result from the magnetization-flop phenomenon [9-12]. In the simple Stoner-Wohlfarth model, where the total energy consists of the Zeeman energy and the exchange coupling between the two Co layers, it was shown in a SyAF that the reduction in the Zeeman energy is always greater than the increase on the interlayer antiferromagnetic exchange coupling as long as the deviation from antiparallel alignment of the Co layers is small [10]. This indicates that, whenever a magnetic field is applied to a SyAF, the magnetization direction of the Co layers is not completely antiparallel, but is deviated toward the applied field direction. Furthermore, the Zeeman energy reduction is greatest when the magnetization directions of the Co layers are orthogonal to the applied field in the film plane. This essentially gives a SyAF an effective uniaxial anisotropy with the easy axis being perpendicular to the applied field, and provides a driving force for magnetization flop. Obviously, the occurrence of magnetization flop is very harmful to MRAM devices because MTJs are no longer in a bi-stable state with different resistances, which is necessary for storing digital information. In the case of a complete magnetization flop where the magnetization directions of the two Co layers are orthogonal to that of the free layer, no change in resistance accompanies the free layer switching.

Only a few articles have been published dealing with magnetization flop since the first theoretical prediction by Zhu and Zheng [10], and all the previous work has been confined to spin-valve multilayers. Zhu and Zheng examined the effects of the aspect ratio and the unidirectional pinning strength by an AF on the rigidity of a SyAF in a full micromagnetic model by using the LLG equation. They observed, in a 0.5 μm × 0.5 μm cell, a very small threshold field of 40 Oe for magnetization flop which is even smaller than the switching field of the free layer. The rigidity of a SyAF, however, was found to be improved by increasing the aspect ratio and by introducing a unidirectional pinning field by using an AF. The first experimental observation of magnetization flop was reported by Tong et al. [9] in spin valves which were exchange-biased by using pinned SyAFs (CoFe/Ru/CoFe/IrMn). Magnetization flop was also observed in post field-annealing experiments by changing the magnitude and the direction of the applied magnetic field and by Marrows *et al.* [11] during sputtering under an applied magnetic field (200 Oe) by simply changing the relative thicknesses of the two Co layers in the SyAF.

In MTJs exchange-biased by SyAFs, the magnitude of the stray field reaching the free layer (and, hence, its bias field) is expected to vary with the relative thickness of the Co layers, and this is one of the two subjects of the present investigation. Additionally, the size effects of the bias field and the coercivity are systematically examined in order to better understand the switching properties of small-sized MTJs which are suitable for high density MRAMs. The other subject of this work is to examine how the rigidity of SyAFs is affected by various magnetic parameters and by the cell size. Particular emphasis is given to cell-size effects due to their importance in high-density MRAM devices.

2. Model and Computation

2.1. Switching characteristics of the free layer

In the model, each magnetic layer consisted of a single domain, indicating that the magnetization was uniform within a layer. The structure of the MTJs modeled in this work was NiFe (I) (7.5 nm)/AlO_x (0.7 nm)/Co (I) (y nm)/ Ru (0.7 nm)/Co (II) (7-y nm)/FeMn (10 nm)/ NiFe (II) (4 nm). This multilayer structure, shown in Fig. 1, was previously investigated by Parkin *et al.* [3]. The relative thickness of the Co layers was changed by varying the value of y from 1 to 6. In order to examine the size effects, multilayers with various dimensions were investigated; namely, 0.8×0.4, 1.2×0.6, 2.8×1.4, 4×2, 6×3, 8×4, 11.2×5.6 and 16×8 (all dimensions in mm). Note that the aspect ratio (defined by the ratio of the length to the width) of all the MTJs was fixed at 2.

The uniaxial induced anisotropies in the free layer (H_{Py}) was 5Oe, and that in the Co layers (H_{Co}) were 20 Oe [3, 5]. The ferromagnetic exchange coupling (more specifically, the Neel orange-peel coupling, the origin of which is magnetostatic interactions in nature) between the free layer and the Co layer next to the AlO_x layer (H_{bias}) was 26 Oe. These magnetic parameters are relevant to the MTJs reported by Parkin *et al.* [3]. The two Co layers separated by a thin Ru layer was antiferromagnetically coupled, and the magnitude of the antiferromagnetic coupling (H_{anti}), which was estimated from the interlayer exchange coupling of -1 erg/cm^2 at the present interlayer separation (0.7 nm) [13], was -1200 Oe. The exchange coupling between the Co (II) and the FeMn layers (H_{pin}) was assumed to be 1200 Oe, which was much higher than the reported values of 400~500 Oe [3, 8] obtained in this type of AF layer. This was to avoid the so-called magnetization-flop behavior observed in SyAFs [9-12] and a subsequent complication of magnetization behavior. The high exchange bias field, combined with the large antiferromagnetic exchange coupling in the SyAF

layers, essentially fixed all the magnetic layers, except for the free layer, during the field cycle. Since one of the main objectives was to examine the magnitude of the stray field reaching the free layer (and hence, its bias field) from the rest of the magnetic layers, the assumption of a high exchange coupling field will not affect the main conclusion of the present work.

The magnetization direction of the two magnetic layers (Co(II) and NiFe(II)) sandwiching the FeMn layer was set to be in the +x direction. This determined the magnetization direction of the Co(I) layer through antiferromagnetic exchange coupling and that of the NiFe(I) (free) layer through orange-peel coupling under the conditions of no magnetostatic interactions (namely, very large cell dimensions) and zero applied field; specifically, the magnetization directions of both the Co(I) and the free layers point in the −x direction. The magnetization direction of all the magnetic layers is also shown in Fig. 1. In this magnetization configuration, the orange-peel coupling biases the free layer, which is the main interest of this work, to the positive direction since the coupling gives the free layer a torque of 26 Oe in the negative direction. It is noted that the bias field direction of the magnetic layer is opposite to the unidirectional torque applied to the layer. A good example is the exchange bias in AF/F (ferromagnet) bilayers. Exchange coupling between the two layers is usually set by first annealing the bilayers well above the Neel temperature of the AF and subsequently cooling them with an applied field on. In this case, the shift in the loop is in the opposite direction to the setting field. The magnetization of the NiFe (more specifically, $Ni_{60}Fe_{40}$) layers was taken as 1055 emu/cm^3 and that of Co as 1400 emu/cm^3 [14]. The magnetic field was applied in the length direction (the same as all the anisotropy fields) and was cycled between +500 and −500 Oe.

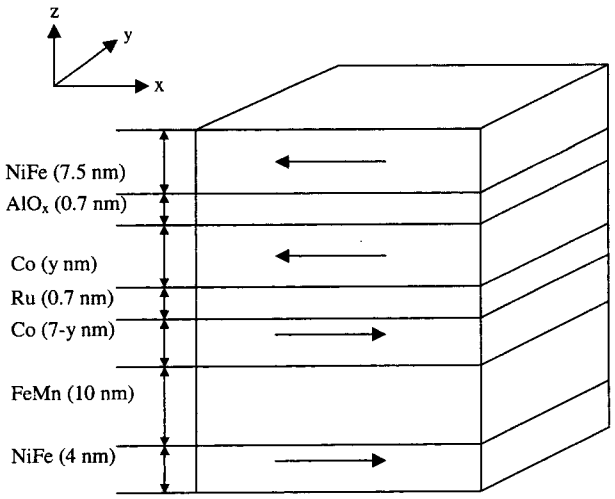

Fig. 1. MTJ structure modeled in this work. The magnetization direction indicated in the ferromagnetic layers is for conditions of no magnetostatic interactions and zero applied field.

2.2. Magnetization flop

The single-domain multilayer model was also used for magnetization flop. The structure of the MTJs modeled in this work was NiFe(I) (7.5 nm)/AlO_x (0.7 nm)/Co(I) (3.5 nm)/Ru (0.7 nm)/Co(II) (3.5 nm)/FeMn (10 nm) (see Fig. 1 for a schematic illustration). A similar structure was previously investigated by Parkin *et al.* [3]. The cell dimensions and the magnetic parameters, such as H_{Py} (5 Oe), H_{Co} (20 Oe), and H_{bias} (26 Oe), are identical to those for the switching-characteristic investigation described in 2.1. The magnitude of the antiferromagnetic coupling field between the two Co layers separated by a thin Ru layer (H_{anti}) varied from −600 to −1200 Oe (the negative sign indicates antiferromagnetic coupling), although it is estimated to be approximately −1200 Oe at the present interlayer separation [13]. The widely varying values of H_{anti} may reflect variations in the surface properties and/or the Ru thickness in real experiments. The exchange coupling between the FeMn and the Co(II) layers (H_{pin}) also varied widely from 0 to 800 Oe. All the uniaxial and unidirectional anisotropies were formed in the length (x) direction. The magnetization direction of Co(II) was set to be in the +x direction. This determined the magnetization direction of the Co(I) layer through the antiferromagnetic exchange coupling and that of the free layer through the orange-peel coupling under the conditions of no magnetostatic interactions (namely, very large cell dimensions) and zero applied field. Specifically, the magnetization directions of both the Co(I) and the free layers pointed in the −x direction (see Fig. 1). In this magnetic configuration, the orange-peel coupling biases the free layer to the positive direction since the coupling gives the free layer a torque in the negative direction. The magnetization of the NiFe (more specifically, $Ni_{60}Fe_{40}$) layer was taken as 1055 emu/cm^3, and that of Co as 1400 emu/cm^3 [14]. The applied magnetic field (H_a) pointed in the length direction (the same as all the anisotropy fields). The maximum applied field during the field cycle was suitably varied in accordance with the magnetic parameters of the multilayers.

3. Results and Discussion

3.1. Switching characteristics of the free layer

The bias field (or offset field) of the free layer, which was obtained from the M-H hysteresis loops, is defined as the center of the hysteresis loop. The bias field is the vector sum of the orange-peel coupling field (+26 Oe) and the interlayer magnetostatic interaction field [7]. In Fig. 2 are shown the results for the relative Co-layer thickness (y) dependence of the bias field of the free layer for varying cell sizes.

A common and prominent tendency is that the magnitude of the bias field decreases with increasing y for all cell sizes. Since the interlayer magnetostatic interaction field in the positive (negative) direction causes a negative (positive)

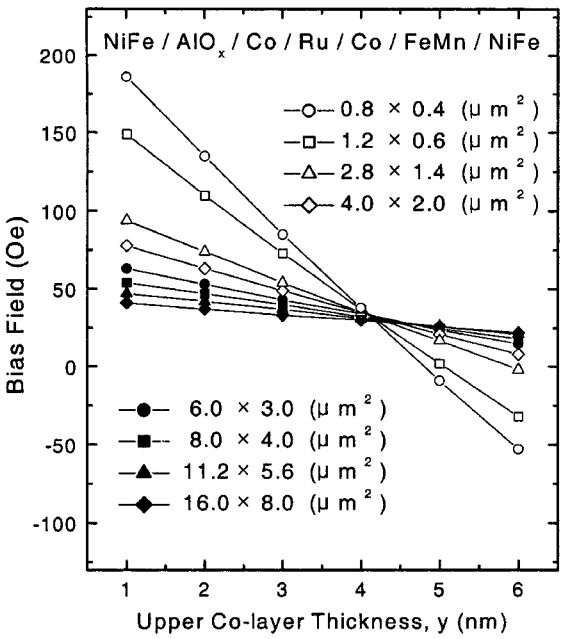

Fig. 2. Bias field as a function of the relative Co-layer thickness in the SyAF for various cell sizes.

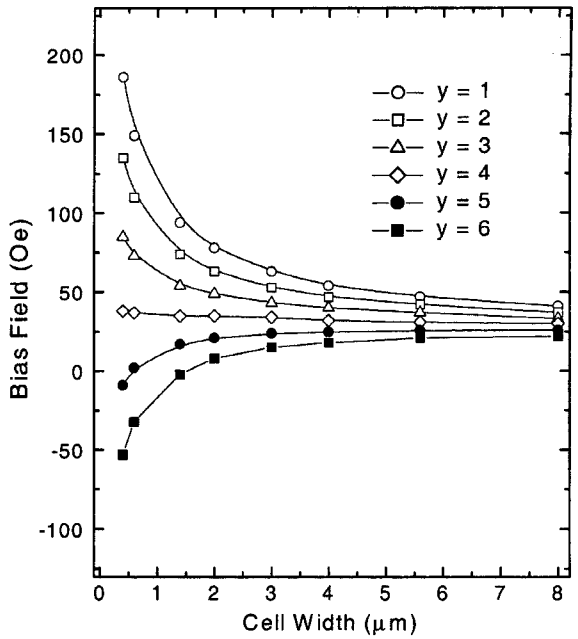

Fig. 3. Bias field as a function of the cell size for various values of y. The cell size is indicated by the cell width.

bias field, the present results indicate that the interlayer magnetostatic interaction field increases in the positive direction with increasing y. This can be understood from the respective contribution of the two Co layers in the SyAF layers to the bias field of the free layer. The contribution of the upper Co layer is expected to be greater, it being closer to the free layer. The interlayer magnetostatic interaction field from the upper Co layer, whose magnetization direction is in the −x direction, points in the +x direction, and its magnitude increases with increasing y since the interlayer magnetostatic interaction field from a neighboring magnetic layer is proportional to the product of the thickness and the saturation magnetization of the layer [7].

With the same saturation magnetization for the two Co layers in the SyAFs, this relationship explains the observed linear decrease of the bias field with y. The contribution of the lower Co layer is exactly opposite to that of the upper layer; the direction of the interlayer magnetostatic interaction field is in the −x direction, and the magnitude decreases with increasing y. The net result is, therefore, an increased interlayer magnetostatic interaction field in the positive direction, and hence, a decreasing bias field with increasing y. The dependence of the bias field on y is relatively small in the case of large cell sizes, but this dependence becomes very large at small cell dimensions. In the largest cell size of 16 μm × 8 μm, for example, the bias field changes from 41 to 22 Oe as y increases from 1 to 6, giving the interlayer magnetostatic interaction fields from −15 to +4 Oe. In the case of the smallest cell size of 0.8 μm × 0.4 μm, the bias field varies from 186 to −53 Oe, resulting in the interlayer magnetostatic interaction fields in the range of −161 to +79 Oe. This clearly indicates the dominant role of the magnetostatic interactions at small cell sizes; at the extreme y values, the shift of the hysteresis loop is 3.0 (y = 6) to ~6.2 (y = 1) times greater than the "intrinsic" orange-peel exchange coupling.

It is worth noting from Fig. 2 that, at y = 4, the cell size dependence of the bias field is extraordinarily small, but the dependence increases as the relative Co-layer thickness deviates from y = 4. The results shown in Fig. 2 are re-plotted in order to show more clearly the cell-size dependence of the bias field at various y values, and these results are shown in Fig. 3. In the figure, the cell size is indicated by the width. Indeed, at y = 4, the size dependence of the bias field is very small, the bias field ranging from 30 to ~38 Oe over the whole size range. However, at other y values, the size dependence of the bias field is large, particularly at cell sizes below 6 μm × 3 μm. A noticeable feature is that the size dependence of the bias field at y = 3 and 5 and the size dependence at y = 2 and 6 are rather symmetric with respect to y = 4 over the whole size range. This symmetry is due to the fact that the interlayer magnetostatic interaction field (and hence, the bias field) is linearly proportional to the thickness of the Co layers in the SyAFs.

It would be of interest to examine the contribution of each magnetic layer to the total interlayer magnetostatic interaction field acting on the free layer, and some of the results are shown in Fig. 4 for y = 4 where the size dependence of the bias field is smallest. Expectedly, the contribution from the upper Co layer, which is thicker than the lower Co layer and closest to the free layer, is largest, and its direction is positive. On the other hand, the contribution from the lower Co layer is negative, and its absolute magnitude is smaller. This indicates that the net contribution

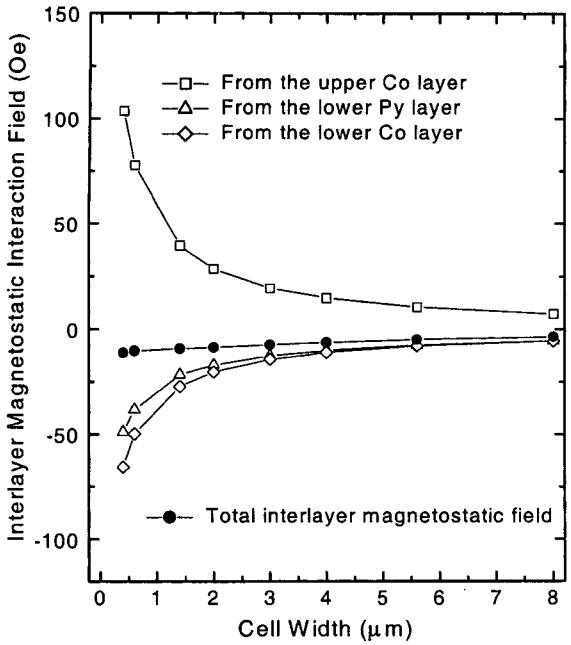

Fig. 4. Contribution of the interlayer magnetostatic interaction field acting on the free layer from neighboring ferromagnetic layers as a function of the cell size. The cell size is indicated by the cell width.

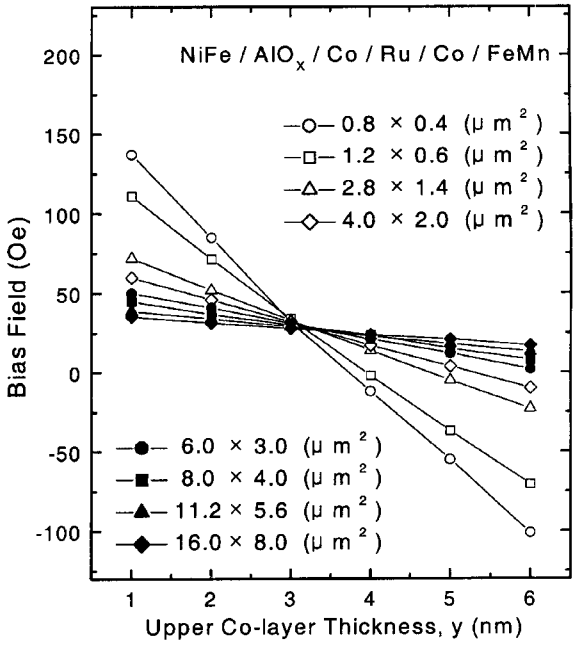

Fig. 5. Bias field for the MTJs without the lower permalloy layer as a function of the relative Co-layer thickness in the SyAF for various cell sizes.

from the two Co layers is positive. However, a nearly constant bias field over the whole size range is seen due to the negative contribution from the lower permalloy layer, whose magnitude is just slightly smaller than that of the lower Co layer. The substantial contribution from the lower permalloy layer is rather unexpected, considering its large distance from the free layer and its small saturation magnetization. This result emphasizes that the contributions from all the magnetic layers must be taken into account in controlling the bias field. With the large contribution from the lower permalloy layer, the dependence of the bias field on the relative Co-layer thickness for the multilayer without the permalloy layer is expected to be different from those shown in Fig. 2. This is actually the case, as can be seen from the results shown in Fig. 5. The overall tendency is the same, but the smallest size dependence is not achieved at y = 4, but at y = 3.

Actual hysteresis loops at some sizes are shown in Fig. 6 in order to show more clearly the switching characteristics of the free layer, which depends on both the bias field and the coercivity. The results are for y = 3, where the cell size dependence of the bias field is moderate and experimental results are available [3]. The loops are completely square shape, indicating that the magnetization change is due to complete spin-flip. This can be expected, since the cell is in a single-domain state, and all the anisotropies (both uniaxial and unidirectional) are parallel or antiparallel to the applied field during the field cycle. The high (low) magnetization state corresponds to the free layer spin direction in the +x (–x) direction. Since only the free-layer magnetization switches in the present field cycle and the pinned layer magnetization is fixed in the x direction, the junction resistance is large (small) at the high (low) magnetization state. A significant increase in the coercivity is observed with decreasing cell size, even though the aspect ratio is fixed at 2. At the largest cell size of 16 μm × 8 μm, the coercivity is 11 Oe, but it is increased to 102 Oe at the smallest cell size of 0.8 μm × 0.4 μm. It was shown previously that the coercivity is the sum of the "intrinsic" uniaxial anisotropy (5 Oe in this case) and the shape anisotropy, which is equal to the difference of the self-demagnetizing fields along the two principal axes (the length and the width directions in this case) [7]. Again, similarly to the bias field, the dominant factor is the magnetostatic interactions at small cell sizes, the calculated coercivity being much greater than the intrinsic value. Also shown in Fig. 6 are the hysteresis loops obtained experimentally by Parkin *et al.* [3]. The original data of Parkin *et al.* were R-H curves (R: junction resistance), but these curves are converted into M-H curves. During the conversion, the magnetization is adjusted so that the experimental magnetization values are equal to the calculated ones at both ends of the applied field (±300 Oe). This data adjustment will not affect the switching characteristics, namely, the bias field and the coercivity. The results for the size dependences of the bias field and the coercivity obtained from the model calculations are compared in Figs. 7(a) and (b), respectively, with those obtained experimentally by Parkin *et al.* [3]. It is seen from Figs. 6 and 7 that the results calculated from the simple single-domain model significantly overestimate both the bias field and the coercivity, although they are in qualitative agree-

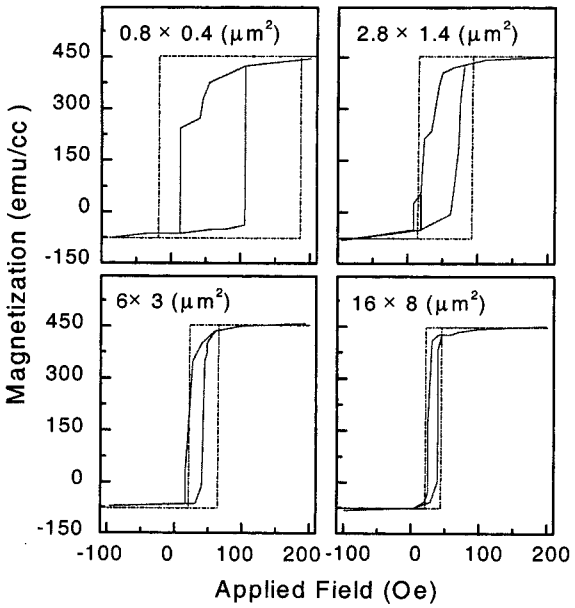

Fig. 6. Hysteresis loops at some cell sizes calculated in this work (broken lines) and measured experimentally by Parkin *et al.* [3] (solid lines). The results are for y = 3.

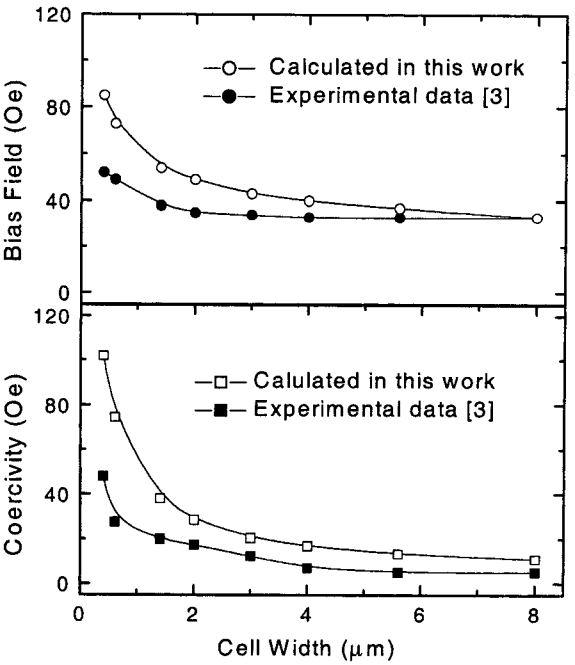

Fig. 7. (a) Bias field and (b) coercivity as functions of the cell size for the MTJ with y = 3. The calculated results are compared with those obtained experimentally by Parkin *et al.* [3].

ment with the experimental results. Actually, the bias field and the coercivity calculated from the single-domain model give upper limits for a given multilayer structure since the magnetostatic energy is highest in a single-domain state. Obviously, the main reason for this discrepancy results from the fact that a real MTJ does not have a single-domain structure, but a multi-domain structure in a way to reduce the magnetostatic interaction energy. Resultantly, the magnetization change occurs not only due to coherent spin rotation but also due to incoherent spin rotation and even domain-wall motion. Another source of discrepancy may be the irregularity of the cell surface formed during the microfabrication process (such as etching). This surface irregularity can cause a complicated domain structure, which may be responsible for the rather complicated hysteresis loops observed in some cells, as shown in Fig. 6. It seems that the hysteresis loops become more complicated at smaller cell sizes. This can be understood from the fact that the surface irregularity effect becomes greater at smaller cell sizes.

From the hysteresis loops shown in Fig. 6, it is worth noting that, as the cell size decreases, the change in the switching field from the low-magnetization state to the high one is much greater than that for the opposite direction. A similar behavior was observed in a previous work [7], where the size dependence of the switching field was found to be much greater when the spin structure changed from a stable state to a less stable one. In a conventional spin valve with two ferromagnetic layers (the free and pinned layers), it is obvious that the stable spin state is when the two spins are antiparallel. The identify the stable spin state is not that obvious, however, when a multiplayer, such as the present one, consists of many ferromagnetic layers. From the size dependence of the switching field, it is thought that the low magnetization state, where the magnetization directions of both the free and the Co(I) layers are parallel and point in the −x direction, is more stable than the high magnetization state. This result can be expected since the magnetization directions of the rest of the magnetic layers point in the +x direction.

3.2. Magnetization flop

From a simple energy consideration, magnetization flop should occur on applying a magnetic field to an SyAF. However, magnetization flop only occurs at magnetic fields greater than a threshold field (H_{th}) due to the energy barrier to the flop. During a field cycle where the maximum applied field is smaller than H_{th}, the magnetization directions of all the layers are always completely parallel or antiparallel, resulting in very simple M-H and MR-H hysteresis loops, as shown in Fig. 6, and a maximum MR change accompanying the free-layer switching. This situation is ideal for MRAM applications. When magnetization flop occurs, the magnetic configuration becomes complicated, causing complicated M-H and MR-H loops. Two main factors are responsible for the complicated M-H and MR-H loops. One is, of course, magnetization flop. The other is related to the fact that the magnetization of the two Co layers in the SyAF scissor toward the axis of the applied field. The latter factor is responsible for the linear changes of magnetization and MR as functions of the applied field. Eventually, the magnetization directions of the two Co layers are expected to be parallel at saturation field where MR is lowest (zero), which corresponds to the points a and i in

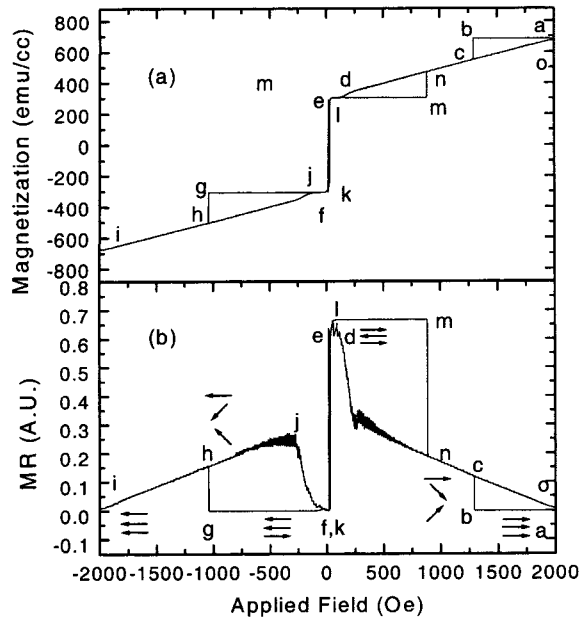

Fig. 8. (a) M-H and (b) MR-H hysteresis loops for a cell size of 16 μm × 8 μm at a maximum applied field of 2000 Oe, which is above the threshold field for magnetization flop. The results are obtained for $H_{bias} = 26$ Oe, $H_{Py} = 5$ Oe, $H_{anti} = -1000$ Oe, $H_{Co} = 20$ Oe, and $H_{pin} = 0$. The magnetic configurations at some important points during the field cycle are also illustrated in (b).

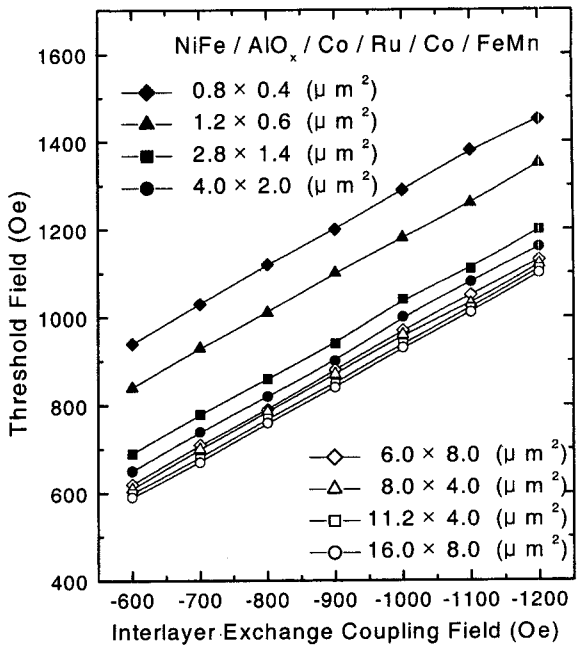

Fig. 9. Threshold field as a function of the antiferromagnetic exchange coupling strength for various cell sizes. The results are obtained for $H_{bias} = 26$ Oe, $H_{Py} = 5$ Oe, $H_{Co} = 20$ Oe, and $H_{pin} = 400$ Oe.

Figs. 8. In order to better understand the magnetic configuration during the field cycle, the magnetization direction of each letter is also illustrated in Figs. 8 (a) and (b). The parallel alignment is maintained until b, below which magnetization-flop occurs (point c). This change occurs abruptly; so does the change in M and MR. An important change at this point is that the two Co layers in the SyAF are aligned antiparallel due to H_{anti}. The antiparallel alignment, however, is far from complete at point c, but it improves with decreasing H_a. As the magnitude of H_a decreases from c to e, M continuously decreases nearly linearly due to the improvement in the antiparallel alignment, but this is not the case for the MR-H curves where a large fluctuation is observed (at around d) and an abrupt change in MR occurs as H_a varies from d to e. In the present model, the change in MR is solely dependent on the angle between the free and the Co(I) layers. With a small-coercivity free layer, the magnetization always points in the +x direction in this H_a range, so MR depends on the magnetization direction of Co(I). Even in the magnetization-flop state, the magnetization direction of Co(I) is not orthogonal to H_a, but is directed toward the H_a direction when H_a is large. As H_a decreases from c to d, the angle between Co(I) and H_a approaches 90°; hence, MR increases. The large fluctuation in MR observed at d (and also j) is related with the orthogonally relationship between the magnetization directions in the SyAF and H_a where a small rotation of the SyAF causes a large change in MR. The sudden jump in MR from d to e is due to the disappearance of the magnetization flop. This clearly demonstrates that magnetization flop is driven by H_a (the Zeeman energy). Thus, the change in M and MR near $H_a = 0$ is similar to the case of no magnetization flop where the change is dominated by the free- layer switching. The conventional SyAF structure is stable (more precisely, metastable) as H_a increases in the –x direction from f to g, where magnetization flop occurs again. With further increases in H_a in the –x direction, the magnetizations of the two Co layers in the SyAF scissor toward the x direction, and the subsequent change in M and MR can be explained. The sudden decrease of MR from j to k is also due to the disappearance of magnetization flop as H_a approaches zero, to the path from d to e. The change in M and MR along the path l → m → n → o can be explained similarly to the one along the path f → g → h → i.

Let us now examine the effects of the magnetic parameters and the cell size on the rigidity of the SyAF. In Fig. 9 are shown the results for H_{th} as a function of H_{anti} for all the cell sizes investigated in this work. The results are obtained for $H_{bias} = 26$ Oe, $H_{Py} = 5$ Oe, $H_{Co} = 20$ Oe, and $H_{pin} = 400$ Oe. The magnitude of H_{th}, above which magnetization flop occurs during the field cycle, was determined by scanning the maximum applied field in steps of 10 Oe. For all the cell sizes, the value of H_{th} increased linearly with increasing H_{anti}. This indicates that H_{anti} plays an effective role in resisting magnetization flop. If the magnetizations of the two Co layers in the SyAF are completely antiparallel, the torques on the two Co layers will be identical, but opposite. This makes it hard for magnetization flop to occur since the torque (or rotation) of one Co layer is exactly counteracted by that of the other. The present results for the effects of

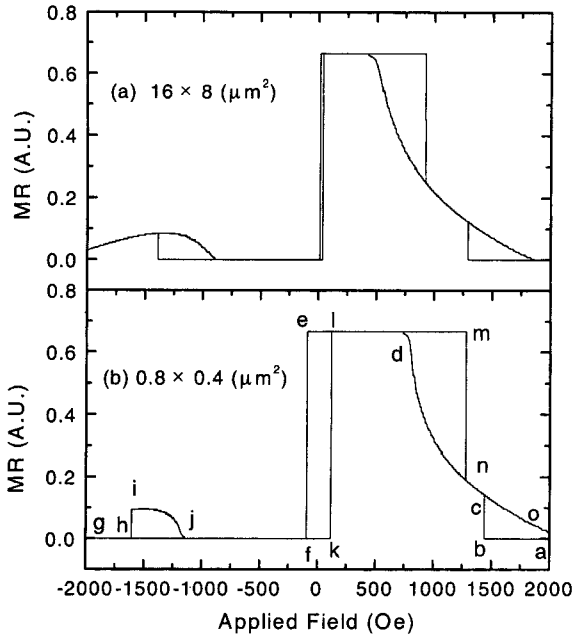

Fig. 10. MR-H hysteresis loops for the two extreme cell sizes of (a) 16 μm × 8 μm and (b) 0.8 μm × 0.4 μm. The results are obtained for H_{bias} = 26 Oe, H_{Py} = 5 Oe, H_{anti} = −1000 Oe, H_{Co} = 20 Oe, and H_{pin} = 400 Oe.

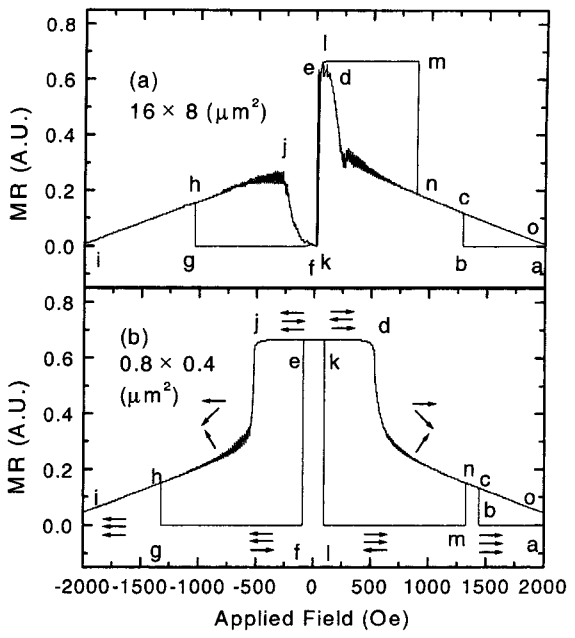

Fig. 11. MR-H hysteresis loops for the two extreme cell sizes of (a) 16 μm × 8 μm and (b) 0.8 μm × 0.4 μm. The results are obtained for H_{bias} = 26 Oe, H_{Py} = 5 Oe, H_{anti} = −1000 Oe, H_{Co} = 20 Oe, and H_{pin} = 0 Oe. The magnetic configurations at some important points during the field cycle are also illustrated in (b).

H_{anti} on the rigidity of the SyAF, shown in Fig. 9, can be explained by a change in the strength of antiparallel alignment as a function of H_{anti}. At a smaller value of H_{anti}, the deviation from a completely antiparallel alignment is greater; hence, a smaller rigidity exists. It is worth noting that the slopes of the H_{th} *vs.* H_{anti} curves are identical for all the cell sizes. The slope is 0.85 in the present model, indicating that the increase in H_{th} is 85% of that in H_{anti}.

The dependence of the resistance to magnetization flop on the cell size is shown in more detail in Figs. 10(a) and (b) where MR-H hysteresis loops are presented for the two extreme cell sizes of 16 μm × 8 μm and 0.8 μm × 0.4 μm, respectively. A comparison of the two loops clearly shows a significant increase in the coercivity of the free layer for the small cell size, which can also be explained by an increase in the shape anisotropy with decreasing cell size. Another important feature is that the H_a range over which the conventional SyAF structure is stable (in other words, no magnetization flop occurs) is large for the small cell size; specifically, the H_a range is from −1388 to 926 Oe for the 16 μm × 8 μm cell while it is from −1607 to 1281 Oe for the 0.8 μm × 0.4 μm cell. Note that magnetization flop occurs at significantly higher values of H_a in the −x direction, because the Co(II) layer is pinned in the +x direction at a strength of 400 Oe by the AF layer.

A rather substantial change occurs in the dependence of the hysteresis loops on H_{pin}, as can be seen from the results shown in Figs. 11 (a) and (b) for the two extreme cell sizes of 16 μm × 8 μm and 0.8 μm × 0.4 μm, respectively. The magnetic parameters used are identical to those used for Figs. 10 (a) and (b), except that H_{pin} = 0 in this case (H_{pin} = 400 Oe for the results shown in Figs. 10(a) and (b)). Thus, by comparing the results shown in Figs. 10 (a) and (b) with those in Figs. 11(a) and (b), one is able to see the difference in MR-H behavior for different values of H_{pin}. A comparison of the MR-H loop shown in Fig. 11(a) with that in Fig. 10(a) for the large cell size indicates that the stability region for the conventional SyAF structure is narrowed in the absence of H_{pin}. In particular, the reduction in the negative direction is substantial, and this can be understood from the direction of H_{pin}, already mentioned in the previous paragraph. A more prominent difference, however, is the significant reduction of the stability region for the SyAF structure, once magnetization flop occurs. This can be seen from the magnitude of H_a at which the magnetization flop transforms into the conventional SyAF structure. In the case of H_{pin} = 0, once magnetization flop occurs, that state prevails since the transformation from magnetization flop into the conventional SyAF structure only occurs near H_a = 0. However, the magnetization-flop state returns to the normal SyAF structure at high H_a values in the presence of H_{pin}. At H_{pin} = 400 Oe, for example, the values of H_a at which the magnetic configuration transforms between magnetization flop and the SyAF structure are −895 Oe and 430 Oe.

A much more striking difference is observed at small cell sizes and H_{pin} = 0. For these conditions, a totally different MR-H hysteresis loop is observed, as can be seen in Fig. 11(b). The loop is now nearly symmetric with respect to $H_a \approx 0$. Cell sizes of 2.4 μm × 1.2 μm and below exhibit this type of hysteresis loop. The main difference is that the MR

change accompanying the free layer switching is identical (from the high MR state to zero) irrespective of the direction of the free-layer switching. In conventional SyAF-type MTJs, however, the MR change is opposite when the direction of the free-layer switching is opposite. The reason for this strange hysteresis loop is the large contribution of the magnetostatic energy to the total energy at small cell dimensions; in particular, a large interlayer magnetostatic interaction field from the free layer determines the magnetization direction of Co(I), the nearest neighbor magnetic layer (and hence, Co(II) through strong antiferromagnetic coupling), in a way to minimize the dominant magnetostatic energy. Specifically, when the magnetization-flop state transforms into the normal SyAF structure (points d and j in Fig. 11(b)), the magnetization direction of Co(I) is aligned antiparallel to that of the free layer, which is parallel to H_a due to the small coercivity. This always results in a high MR state before free-layer switching. A similar behavior is expected to occur at small values of H_{pin}. The magnetization directions of all the magnetic layers are indicated at some important points in Fig. 11(b). After free-layer switching, the magnetization direction of the free layer is parallel to that of Co(I), which significantly increases the magnetostatic energy. However, this state is maintained up to high H_a values due to the large shape anisotropy (and hence, coercivity) of the Co layers, which provides a large resistance to magnetization flop, as was discussed earlier.

4. Conclusions

Computer simulations using a single-domain multilayer model have been carried out in this work to investigate the switching characteristics and the magnetization-flop behavior in magnetic tunnel junctions field in magnetic tunnel junctions exchange-biased by Co/Ru/Co synthetic antiferromagnets. A linear change of the bias field is observed as a function of the relative Co-layer thickness, and the change is found to be greater at smaller cell dimensions due to a larger interlayer magnetostatic interaction field. The bias field of the free-layer remains nearly unchanged with the cell size at a certain Co-layer thickness due to a balance of the stray field contribution from neighboring ferromagnetic layers. The coercivity is observed to increase significantly with decreasing cell size, and the coercivity at small cell dimensions is dominated by magnetostatic interactions, the calculated coercivity being much greater than the intrinsic value. The values calculated from the present simple model overestimate the bias field and the coercivity, but the calculated hysteresis loops are in qualitative agreement with the experimental results. The change in the switching field from the low magnetization state to the high one is much greater than that for the opposite direction, indicating that, unlike a conventional simple spin-valve, the low magnetization state with the magnetization directions of both the free and the upper Co layers aligned parallelly is more stable than the high magnetization state.

The magnetization-flop behavior occurs above a threshold field. As the cell size is decreased, the resistance to magnetization flop increases due to the increased shape anisotropy, and hence the increased coercivity, of the Co layers in the SyAF. In the case of no or weak pinning of the SyAF, MTJs with small cell dimensions are not suitable for MRAM applications since the MR change accompanying the free-layer switching is always from the high MR state to zero, irrespective of the direction of the free-layer switching. The large interlayer magnetostatic interaction field from the free layer is responsible for this behavior. This emphasizes the importance of strong pinning for SyAFs with small cell dimensions. The resistance to magnetization flop increases linearly with increasing antiferromagnetic exchange coupling between the two Co layers in the SyAF because, for a given applied field, the deviation from a complete antiparallel alignment is higher at a smaller exchange coupling. The transition from magnetization flop to the normal SyAF structure, which is in a direction opposite to that of the magnetization flop, occurs at high (low) H_a values when the resistance to magnetization flop is high (low). Irrespective of the magnetic parameters and the cell sizes, the magnetization-flop state does not exist near $H_a = 0$, indicating that magnetization flop is driven by the Zeeman energy.

Acknowledgments

The simulation was performed with a program developed at National Institute of Standards and Technology by Dr. John Oti (now at Euxine Technologies). Financial support from the Tera-level Nanodevices Project (a 21C Frontier Program Funded by the Korean Ministry of Science and Technology) is gratefully acknowledged.

References

[1] D. D. Tang, P. K. Wang, V. S. Speriosu, S. Le and K. K. Kung, IEEE Trans. Magn. **31**, 3206 (1995).
[2] S. E. Russek, J. O. Oti, Y. K. Kim and R. W. Cross, IEEE Trans. Magn. **33**, 3292 (1997).
[3] S. S. P. Parkin, K. P. Roche, M. G. Samant, P. M. Rice, R. B. Beyers, R. E. Scheuerlein, E. J. O'Sullivan, S. L. Brown, J. Bucchigano, D. W. Abraham, Yu Lu, M. Rooks, P. L. Trouilloud, R. A. Wanner and W. J. Gallager, J. Appl. Phys. **85**, 5828 (1999).
[4] S. Tehrani, J. M. Slaughter, E. Chen, M. Durlam, J. Shi and M. DeHerrera, IEEE Trans. Magn. **35**, 2814 (1999).
[5] J. S. Moodera and G. Mathon, J. Magn. Magn. Mater. **200**, 248 (1999).
[6] X.-F. Han, M. Oogane, H. Kubota, Y. Ando and T. Miyazaki, Appl. Phys. Letters **77**, 283 (2000).
[7] S. H. Lim, S. H. Han, K. H. Shin and H. J. Kim, J. Magn. Magn. Mater. **223**, 192 (2001).
[8] J. L. Leal and M. H. Kryder, J. Appl. Phys. **83**(7), 3720

(1998).
[9] H. C. Tong, C. Qian, L. Miloslavsky, S. Funada, X. Shi, F. Liu and S. Dey, J. Appl. Phys. **87**(9), 5055 (2000).
[10] J. Zhu and Y. Zheng, IEEE Trans. Magn. **34**, 1063 (1998).
[11] C. H. Marrows, F. E. Stanley, and B. J. Hickey, J. Appl. Phys. **87**(9), 5058 (2000).
[12] J. G. Zhu, IEEE Trans. Magn. **35**, 655 (1999).
[13] S. S. P. Parkin, N. More and K. P. Roche, Phys. Rev. Letters **64**, 2304 (1990).
[14] S. S. P. Parkin, Proceedings of the International Symposium on Magnetics for the 10th Anniversary of the Korean Magnetics Society (Cheju Island, Korea, September 28-30, 2000), Edited by S. H. Lim, C. S. Kim and T. D. Lee, Hanrim Printing Co., Seoul, Korea.